

Green Chemistry

Accepted Manuscript



This article can be cited before page numbers have been issued, to do this please use: T. Pfennig, J. M. Carraher, A. Chemburkar, R. L. Johnson, A. Anderson, J. Tessonier, M. Neurock and B. H. Shanks, *Green Chem.*, 2017, DOI: 10.1039/C7GC02041D.



This is an Accepted Manuscript, which has been through the Royal Society of Chemistry peer review process and has been accepted for publication.

Accepted Manuscripts are published online shortly after acceptance, before technical editing, formatting and proof reading. Using this free service, authors can make their results available to the community, in citable form, before we publish the edited article. We will replace this Accepted Manuscript with the edited and formatted Advance Article as soon as it is available.

You can find more information about Accepted Manuscripts in the [author guidelines](#).

Please note that technical editing may introduce minor changes to the text and/or graphics, which may alter content. The journal's standard [Terms & Conditions](#) and the ethical guidelines, outlined in our [author and reviewer resource centre](#), still apply. In no event shall the Royal Society of Chemistry be held responsible for any errors or omissions in this Accepted Manuscript or any consequences arising from the use of any information it contains.



Green Chemistry

A new selective route towards benzoic acid and derivatives from biomass-derived coumalic acid

Received 00th January 20xx,
Accepted 00th January 20xx

DOI: 10.1039/x0xx00000x

www.rsc.org/

Toni Pfennig,^{a,b} Jack M. Carraher,^{a,b} Ashwin Chemburkar,^{b,c} Robert L. Johnson,^{a,b} Austin Anderson,^{a,b} Jean-Philippe Tessonnier,^{a,b} Matthew Neurock^{b,c} and Brent H. Shanks^{a,b}

The selective production of aromatics from bio-based sources is an area of interest to expand the potential for greener alternatives to petroleum-derived chemicals. A scalable, efficient route to produce bio-based benzoates is demonstrated in up to 100 mol% yield by carrying out heterogeneous catalytic reactions in non-toxic bio-based solvents at 180 °C. This approach extends the 2-pyrone (coumalic acid/methyl coumalate) Diels-Alder platform by utilizing a bioavailable co-reactant ethylene. A detailed investigation using a combination of kinetic experiments, DFT calculations, and multi-dimensional NMR was carried out to determine the detailed reaction network, and corresponding activation energies for critical steps. Additionally, a series of experiments were conducted to maximize yields by comparing different solvents, for both coumalic acid and methyl coumalate. Our results show that the choice of solvent was a significant factor when coumalic acid was the reactant (yields 71-92 mol%), while methyl coumalate was only minimally affected by the solvent (yields 95-100 mol%). Interestingly, the reaction network and kinetic analysis showed that the Diels-Alder reactions were not significantly different between coumalic acid and methyl coumalate, with the rate limiting step for both being decarboxylation with an activation barrier of 141 kJ/mol compared to 77 kJ/mol for the formation of the bicyclic adduct. Lastly, the reaction cascade was found to be highly susceptible to by-product formation when as little as 5 vol% water was present in the solvent, which demonstrates that the absence of water is essential for high yielding benzoate production.

Introduction

The search for alternatives to fossil-based feedstocks has led to rapid technological advances in the field of bio-renewable chemicals creating many potential opportunities for materials based on renewable carbon sources.¹⁻⁶ Technologies to produce aromatics from biomass-derived sources have become targets of interest due to the expansion of shale gas extraction, which has led to a relatively reduced availability of >C4 building blocks, including aromatics.^{2, 6, 7} Aromatics are among the most important building blocks used by the chemical industry for the production of a wide array of

products, so there is an incentive for the development of selective processes to produce aromatics from bio-based feedstocks.^{2, 6, 7}

Benzoic acid (BA) is a large scale commodity chemical with an annual production of 638 kt⁸ currently produced by the partial oxidation of toluene using a cobalt-manganese catalyst. BA is used in a wide variety of applications including plasticizers, preservatives, dyes/perfumes and as a feed to produce other chemicals including phenol, caprolactam, and benzaldehyde. Hence, a renewable pathway to produce BA would have broad ranging impacts throughout the chemical value chain.

One route to make bio-based BA is through a formic acid mediated dehydration of quinic or shikimic acid produced via fermentation. This process has several desirable features including high yields for the chemical transformation of quinic and shikimic acids into benzoic acid (up to 90%)² and high titers up to 60 g/L for quinic acid and 71 g/L shikimic acid starting from the substrate glucose and using *metabolically engineered E. coli*.^{9,10} Although, the primary drawback of this approach is the intrinsically low maximum theoretical yield of

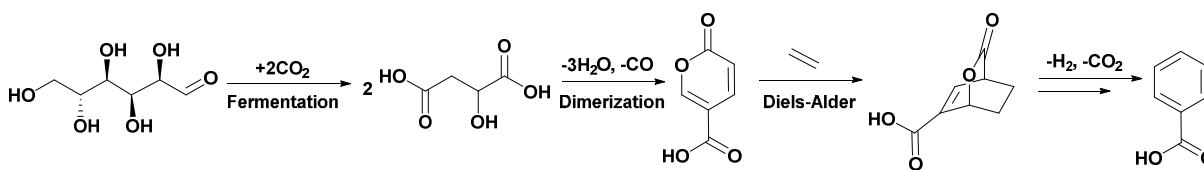
^a Department of Chemical and Biological Engineering, Iowa State University, Ames, IA 50011, USA. E-mail: bshanks@iastate.edu

^b NSF Engineering Research Center for Biorenewable Chemicals (CBiRC), Ames, IA 50011, USA.

^c Department of Chemical Engineering and Material Science, University of Minnesota, Minneapolis, MN 55455, USA

† Electronic Supplementary Information (ESI) available: [details of any supplementary information available should be included here]. See DOI: 10.1039/x0xx00000x

the shikimic/quinic acid fermentation of 43 %, and to date the highest yields reported correspond to an



Scheme 1. The formation of benzoic acid starting from glucose fermentation to malic acid using acid catalysed dimerization to coumalic acid followed by a Diels-Alder/decarboxylation/dehydrogenation reaction sequence to yield the desired aromatics.

overall mol/mol yield of 23, and 27 %.¹⁰ This fermentation bottleneck creates a significant problem for efficient utilization of the glucose feedstock. As a major fraction of the total cost of the fermentation step is the glucose feedstock, its inefficient utilization would have a significant negative impact on the cost required to produce BA.

An alternative pathway to bio-based BA and its methyl ester (MeBA) is through a furanic based platform utilizing a Diels-Alder reaction sequence of furan with methyl acrylate (or acrylic acid) showing moderate yields up to 51 mol%.⁷ Additionally Diels-Alder reactions of methyl furan with ethylene provides a viable pathway to produce bio-based toluene, which could be utilized as a drop-in replacement for production of BA. Toluene selectivities, however, never exceeded 46 mol% due to by-product formation.¹¹ Improvement to this selectivity would require approaches to improve the stability of the bio-based starting materials thereby minimizing by-product formation.

Another approach utilizing biological and chemical catalysis to produce partially biomass-derived methyl benzoate (MeBA) is based on the bio-based cyclic lactone methyl coumalate (MeCMA). The formation of bio-based MeBA is accomplished using a one-pot Diels-Alder/decarboxylation/dehydrogenation reaction sequence between MeCMA and butyl vinyl ether with excellent yields up to 89 mol%.¹²

Bio-based 2-pyrone can be produced by the fermentation of glucose to form malic acid^{13, 14} followed by acid catalyzed dimerization of malic acid to coumalic acid (Scheme 1).¹² The synthesis of 2-pyrone coumalic acid (CMA) via this route has several attractive features. First, the atom efficiency of the malic acid fermentation is highly favorable, with the capability to even utilize a CO₂ fixing pathway allowing for a theoretical yield of 2 moles of malate per mole of glucose (Scheme 1).¹⁴ Second, efficient fermentation technology is already developed for this route. For example, Novozymes currently uses a metabolically engineered *Aspergillus oryzae* capable of producing 1.38 mol malate per mol glucose at a theoretical yield of 69 % and with high titers of 154 g/L, which could be implemented on an industrial scale.¹³

An approach to improve the viability of the 2-pyrone CMA/MeCMA platform is to utilize a less expensive dienophile as the co-reactant. In theory ethylene should work in an analogous fashion as butyl vinyl ether, but at a substantially lower cost with nearly perfect atom efficiency. Additionally, as the production of ethylene from bio-ethanol is commercially demonstrated, a potential exists for 100 % bio-based process.³

As part of the development of new biomass-derived and renewable processes, we report herein report on the synthesis of BA or MeBA from CMA or MeCMA, respectively, and ethylene with very high yields of >91 mol-% utilizing a one-pot sequential Diels-Alder/decarboxylation/dehydrogenation reaction path. Considering the industrial importance of renewable BA, and the lack of available comprehensive information about this alternative route in the literature, the focus of this work is to provide detailed information of the reaction network, and intrinsic kinetics of individual reaction steps, which can be used to improve the overall process.

Results and discussion

The formation of benzoic acid from coumalic acid

Experiments were conducted to examine the BA and MeBA yields obtained in several solvents using either CMA or MeCMA, respectfully. The reaction between CMA and ethylene in a nonpolar solvent, toluene, resulted in 71 mol% yield of BA at 100 mol% CMA conversion (Table 1, Entry 1). This outcome was similar to reported yields (76 %) for the Diels-Alder reaction of CMA with propylene in toluene,^{15, 16} which was thought to be due to CMA being sparingly soluble in toluene leading to a substantial amount of CMA being converted to unidentified by-products. Therefore, a solvent was used to increase the solubility of CMA in order to improve the overall reaction yield. We have previously shown that γ -valerolactone (GVL) is a good polar aprotic solvent for this reaction system due to structural similarities.¹⁶ The use of GVL resulted in only a slightly higher BA yield of 76 mol% (Table 1, Entry 2 and Figure S1). Still, a considerable amount (~24 mol%) of the initial CMA was lost to by-product formation. Results from previous studies suggested that CMA stability was limited in GVL under reaction conditions due to the presence of residual water in GVL.¹⁶ This hypothesis was tested by using the polar aprotic solvents, 1,4-dioxane or acetone, resulting in a significant improvement in the BA yield (Table 1, Entry 3 and 7). The reaction profile of the CMA consumption over time is displayed in Figure S2. At 100 mol% CMA conversion the BA selectivity was 91 mol% after a 4 hr reaction at 180 °C for both solvents. From UPLC-PDA/QDa analysis, it was evident that small amounts of (4) and (6) (see Scheme 2) were present. Additionally, the formation of (4) was verified with NMR analysis showing that roughly 6 mol% of (4) was formed (Table 1, Entry 3). At this reaction temperature, the dehydrogenation reaction was extremely rapid as evident from the lack of an

observable amount of the diene intermediate (3). This result was consistent with previous studies¹⁶ in which we have shown that the dehydrogenation of

Table 1. Conversion of CMA/MeCMA with ethylene to BA/MeBA.

Entry	Reactant	Solvent	Conv.		Selectivity		
			(1) [mol%]	(5) [mol%]	(3) [mol%]	(4) [mol%]	(6) [mol%]
1	CMA	Toluene	100	71	[a]	[a]	[a]
2	CMA	GVL	100	76	[a]	[a]	[a]
3	CMA	1,4-Dioxane	100	91±1.5	[a]	5.8 [d]	[a]
4	MeCMA	Toluene	100	100±2	[b]	[b]	7±2 [c]
5	MeCMA	GVL	100	99±1	[b]	[b]	2±10 [c]
6	MeCMA	1,4-Dioxane	100	95±1	2±7 [c]	2±3 [c]	5±8 [c]
7	CMA	Acetone	100	91	[a]	[a]	[a]

Reaction conditions: Temperature: 180 °C; reaction time: 4 h, starting concentration: 10 mg ml⁻¹ MeCMA/CMA (1) in 1,4-dioxane, reaction volume: 30 ml, pressure: 500 psig ethylene, agitation: 400 rpm, Pd/C catalyst: 100 mg, [a] unable to quantify by-products with UPLC-PDA/QDa, [b] by-products not detected with GC-FID/MS, [c] cyclohexadiene (3) and cyclohexene (6) intermediates were quantified based on methyl benzoate (5) as reference due to the similar FID response factor. Double Diels-Alder by-product (4) was approximated using methyl benzoate (5) as reference material, [d] quantified via ¹H-NMR.

the diene species proceeded significantly faster than the decarboxylation of the bicyclic intermediate, thereby suggesting that the decarboxylation of the cycloadduct was the limiting step in the reaction network.¹⁶ Kinetic studies and DFT calculations corroborate that decarboxylation is the rate limiting step, which will be discussed in the subsequent sections.

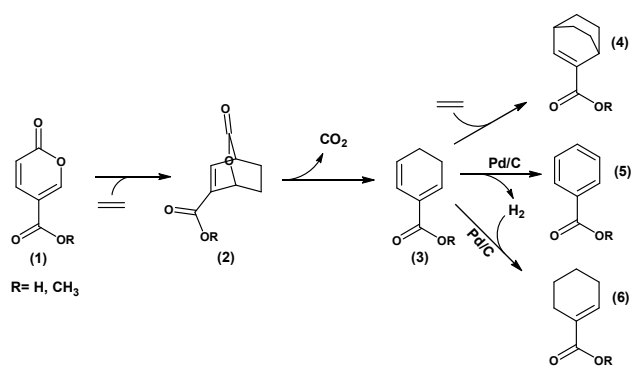
Literature reports suggest that changing the functional group on the starting substrate could significantly influence the stability and reactivity towards Diels-Alder reactions.^{15, 17, 18} This effect was demonstrated by Pacheco et al. using furanic dienes showing different product selectivities when various oxidized versions of HMF were reacted with ethylene, which was purported to be the outcome of different functionalities of the oxygenated furans.¹⁷ Furthermore, Berard et al. observed that the reaction of sorbic acid with ethylene resulted in only low conversion (3 %), while using the ethyl ester of sorbic acid instead, afforded a ~5 fold increase in conversion (14 %).¹⁸ A similar phenomena was also observed with 2-pyrones showing improved yields when reacting MeCMA instead of CMA with propylene.¹⁵

Therefore, reactions were also run using MeCMA as the reactant to determine if starting with the methyl ester of CMA (MeCMA) would alter the reaction. Interestingly, the reaction in toluene showed tremendous improvement in yield with 100 mol% selectivity after complete conversion (Table 1, Entry 4 and Figure S3). The higher selectivity with MeCMA was also consistent with the hypothesis of the importance of the solubility of the starting substrate in the 2-pyrone conversion. Similarly, when the polar aprotic solvent GVL was used to mediate the MeCMA and ethylene reaction, a conversion of 100 mol% with nearly 100 mol% MeBA selectivity (Table 1, Entry 5 and Figure S4) was achieved. As the CMA conversion in GVL only resulted in a selectivity of 76 mol% (Table 1, Entry 2 and Figure S1), the esterification of the carboxylate moiety likely played a significant role in improving the selectivity. Since CMA conversion to BA achieved the highest selectivity in 1,4-dioxane, we also performed the MeCMA conversion in 1,4-dioxane. As shown in Table 1, Entry 6 reported only a slightly better product selectivity (95 mol%) compared to CMA (91

mol%). GC-MS analysis suggested that the remaining five percent was attributed to the unreacted methyl cyclohexa-1,5-diene carboxylate intermediate (3), the formation of methyl cyclohex-1-ene carboxylate (6), and the double Diels-Alder (DDA) by-product (4), which was believed to be the outcome of a consecutive Diels-Alder reaction of (3) with ethylene (Scheme 2). The concentration profile of (1), (2), (3), (4), (5) and (6) over time is displayed in Figure S17. The formation of (2), (3), and (6) were validated via 2D-NMR COSY and HSQC experiments (see Figure S1-S11) and will be explained in detail in the following section.

Elucidating the reaction network

To elucidate where by-product formation was occurring, experiments were performed to determine the reaction network. Given the extensive work on Diels-Alder reactions of 2-pyrones^{12, 19-29} a reaction network was postulated, which is depicted in (Scheme 2). The reaction of CMA/MeCMA with ethylene follows a series of reactions that include Diels-Alder adduct formation (2), decarboxylation of the adduct to yield (3) and a Pd/C catalysed dehydrogenation reaction to form the desired aromatics (5). In the presence of the Pd/C catalyst additional minor products (4) and (6) were observed (Table 1, Entry 6). The formation of (6) is likely the result of a Pd catalysed hydrogenation of (3). The hydrogen needed for this step was likely formed through dehydrogenation of (3) to (5). Data shown in Figure S5 support the proposed reaction network which is evident via the clear trend showing how the conversion of (1) resulted in the formation of intermediates (2) and (3) and small



Scheme 2. Network for the reaction of CMA/MeCMA with ethylene.

amounts (<8 mol%) of (4) and (6) while (5) was formed. Structural identification of the intermediates (2), (3) and by-products (4) were determined by performing 1D and 2D NMR experiments of the reaction products from the MeCMA reaction with ethylene in the absence of catalyst to examine the Diels-Alder/decarboxylation sequence (see Figure S6-S16 and Table S1-S3). These analyses confirmed the formation of (2), (3) and (4). Without the catalyst, the by-product (6) was not observed. Therefore, it appeared that the formation of (6) was only realized when there was formation of hydrogen from dehydrogenation of (4) to (5). Similar observations were made when CMA was used as the starting substrate.

2-Pyrone degradation studies

Loss in selectivity due to MeCMA and CMA degradation was examined. These reactions were performed in the absence of ethylene or catalyst and the results are given in Table 2 and Figures S17-S18. The results are consistent with a previous study¹⁶ showing that CMA stability is compromised in GVL as 25 mol% of the starting material is degraded after 8 h at 180 °C (Table 2, Entry 1). Identical tests in 1,4-dioxane showed that both CMA and MeCMA were significantly more stable with only 3 mol% of MeCMA and 10 mol% of CMA being converted (Table 2, Entry 3 and 4). This observation demonstrated that not only the solvent, but also the state of the starting substrate (acid vs ester) impacts the stability of the 2-pyrone. Given the observed selectivity loss (Table 1, Entry 2, 3 and 6) it appears that CMA breakdown occurs concomitantly while forming (2), thus, impacting the global yield of the desired aromatic product.

In a previous study, it was shown that the presence of small amounts of water accelerated CMA degradation.¹⁶ A similar water mediated breakdown was observed by Chia et al. when the 2-pyrone, triacetic acid lactone (TAL), was exposed to water and heat.³⁰ They report that TAL undergoes ring-opening in the presence of water but is stable in aprotic polar solvents. To determine if the esterified 2-pyrone was more resistant to breakdown due to water, MeCMA stability experiments were also performed in 1,4-dioxane with 5 vol% of water. (Table 2, Entry 6). These results show that esterification did little to prevent breakdown in the presence of water, since both CMA and MeCMA were entirely

consumed. Based on these observations, it is evident that the presence of water in the solvent has to be minimized to maximize yields of the Diels-Alder reaction products.

Overall, GVL is an environmentally friendly renewable solvent with many positive characteristics such as low toxicity and biodegradability³¹⁻³³ and, as such, is a desirable solvent for the conversion of MeCMA to MeBA. However, when BA formation was targeted, the effect of GVL on CMA stability was not as high since 25 mol% of the starting material was lost most likely through a concomitant degradation pathway (Table 1, Entry 2). Moreover, the high boiling point of GVL would make the product separation difficult. As such, a low boiling bio-based acetone solvent could be utilized for increased BA selectivity of 91 mol% and would be an environmentally-advantaged substitute.

Table 2. Degradation of CMA and MeCMA in 1,4-dioxane.

Entry	Reactant	Solvent	CMA Conv. (mol-%)
1	CMA	GVL	25 ¹⁶
2	CMA	GVL + 5 vol% water	100 ¹⁶
3	CMA	1,4-dioxane	10
4	MeCMA	1,4-dioxane	3
5	CMA	1,4-dioxane + 5 vol% water	100
6	MeCMA	1,4-dioxane + 5 vol% water	100

Reaction conditions: Temperature: 180 °C, reaction time: 8 h, starting concentration: 10 mg ml⁻¹ MeCMA/CMA (1) in 1,4-dioxane, reaction volume: 30 ml, pressure: 500 psig N₂, agitation: 400 rpm.

Reaction kinetics of water mediated coumalic acid breakdown

The reaction kinetics and products from the water-mediated breakdown of CMA were determined using NMR analysis with deuterated dioxane-*d*8. Dioxane, an aprotic polar solvent, was chosen as the ideal model system due to minimal by-product formation and CMA/MeCMA degradation. Moreover, fully deuterated dioxane-*d*8 was commercially available allowing the kinetic studies to be performed in a closed system (high pressure NMR tube from Wildmad-Labglass), which simplified the product identification and quantification without further sample workup.

Different D₂O concentration (1-5 vol%) were added to the reaction mixture to identify the CMA breakdown dependence with respect to the water concentration. The main product identified via ¹H NMR after a 6.4 h reaction at 171 °C with 3 vol% D₂O was 2-butenal yielding 14.5 mol% at 25.3 mol% conversion (Figure S19). Minimal 2-butenal was observed with 1 vol% D₂O and virtually none with 0 vol% D₂O. The rate constant for the CMA breakdown reaction, was obtained from initial conversion data (no more than 20 mol% conversion). For each D₂O concentration experiment, a pseudo-first order reaction in CMA was fit to the data. The changes with respect to water in this regime were considered negligible as the reactions were carried out in excess D₂O (e.g. [D₂O] was about 4 times [CMA]₀ at 1 vol% D₂O). Fits of ln([CMA]_t/[CMA]₀) vs time were linear and the observed rate constant (*k*_{obs}) was obtained from the slope. Interestingly, the plot of the pseudo-first order rate constants *k*_{obs} as a function of [D₂O] revealed a

second order dependence on $[D_2O]$ with an independent degradation pathway when no D_2O was added (Figure 1). Therefore, an overall rate law for CMA degradation was expressed as:

$$r_{CMA} = -k_{obs}[CMA] = -(k_1 + k_2 [D_2O]^2)[CMA] \quad (1)$$

The degradation of coumalic acid with and without the presence of water can be captured by the paths shown in Scheme 3. Further insights into the steps and mechanisms responsible for the degradation of CMA to 2-butenal were established by carrying out density functional theory calculations (Scheme 4). The results suggest that water initiated degradation of CMA proceeds via a nucleophilic attack of water on the double bonds in CMA. The intermediate formed (1a) subsequently undergoes ring-opening via keto-

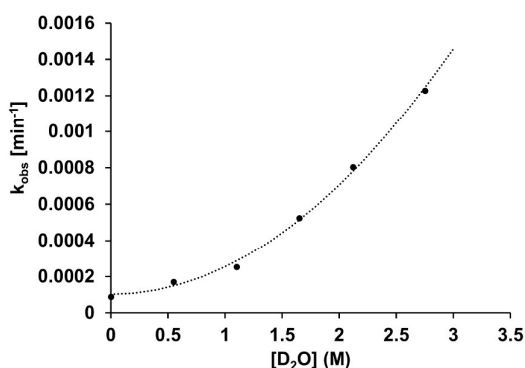
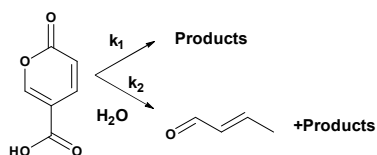


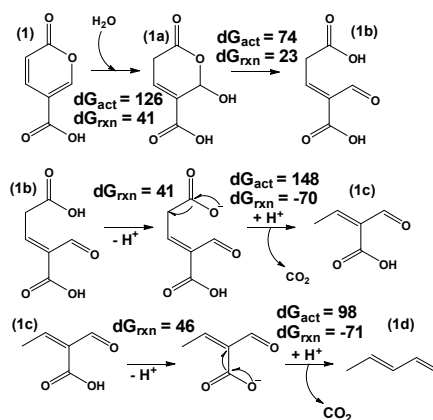
Figure 1. Plot of k_{obs} as a function of $[D_2O]$. Experimentally determined k_{obs} are represented as points and the line is a simulated fit to $k_{obs} = k_1 + k_2 \times [D_2O]^2$ where $k_1 = 1.03 \times 10^{-4} \text{ min}^{-1}$ and $k_2 = 1.51 \times 10^{-4} \text{ M}^{-2} \text{ min}^{-1}$.



Scheme 3. General degradation of coumalic acid in the absence and presence of water.

enol tautomerization to form a keto intermediate (1b). The presence of water molecules facilitates this ring-opening by providing a hydrogen bonding network to enable rapid proton shuttling and a low energy paths for keto-enol tautomerization and ring-opening. The intermediate (1b) has two carboxylic groups, which can then undergo decarboxylation yielding 2-butenal. This is very similar to a previously reported mechanism for water catalysed ring-opening and decarboxylation of triacetic acid lactone.²⁹

To further validate whether CMA breakdown is solely responsible for the observed selectivity loss (Table 1, Entry 2, 3 and 6) or is a result of by-product formation on the pathway to BA, the rate constants of CMA breakdown and CMA Diels-Alder addition with ethylene were compared. Based on the rate constants provided in Figure 1 and calculated from the



Scheme 4. CMA breakdown mechanism to 2-butenal in the presence of water (Units in kJ/mol).

Diels-Alder reaction step (Table S4), it is evident that the CMA degradation proceeds significantly slower (>100 times) than the Diels-Alder addition step. Therefore, the observed loss in product selectivity less likely originates from 2-pyrone breakdown as opposed to by-product formation from intermediates on the pathway to BA. This was further supported by DFT calculations which predicted that the Gibbs free energy of activation barrier for water addition (126 kJ/mol) was ~ 15 kJ/mol higher than ethylene addition (111 kJ/mol). The increase in the barrier is likely due to hydrogen bonding stabilization of the reactant by water. Moreover, the Gibbs free energy of reaction for ethylene addition (-79 kJ/mol) was calculated to be much more exothermic than that for water addition (41 kJ/mol) suggesting that the Diels-Alder adduct is thermodynamically favoured over CMA decomposition. Therefore, it appears that the selectivity loss of 24 mol% originates from intermediates (2) or (3) on the pathway to BA when reacting CMA with ethylene in GVL (Table 1, Entry 2).

Given that reactions performed in dry polar aprotic solvents resulted in selectivities >90 mol% (with <10 mol% known by-products (4) and (6)), it appears that residual water in GVL is responsible for the selectivity loss likely from intermediate (2) or (3). To test this hypothesis, reactions of (2) were performed *in situ* (NMR tubes) in dioxane-*d*8 at 180 °C for 4 h in the presence of 5 vol% D_2O and without a catalyst. The results from these experiments suggest that species in the 1H -NMR spectra are primarily attributed to unidentified by-products meaning that either (2) or (3) is further consumed to unknowns in the presence of water. From this observation, it is clearly critical to avoid water in the system to maximize product yield by minimizing by-product formation from the reactive intermediates.

Reaction kinetics in the absence of catalyst

Kinetic measurements were performed in 1,4-dioxane which is an excellent model solvent for detailed kinetic analyses as it has a low boiling point, results in minimal by-product formation during reaction and is readily available commercially in the fully deuterated dioxane-*d*8 form to perform

complementary *in situ* NMR analysis. Choosing a solvent with a low boiling point (compared to GVL) was critical for isolation, identification and quantification (via NMR) of the temperature sensitive reactant CMA (1) and intermediates (2) and (3) for both the Diels-Alder and decarboxylation reactions. Fully resolved spectra of the formation of (2) and (3) are depicted in Figure 2 showing that the peak assignments and the method of quantification via NMR was unambiguous with carbon balances of >96 mol%.

Diels-Alder reaction step

The activation barrier associated with the formation of the Diels-Alder (DA) adduct (2) was investigated by comparing the rate of consumption of CMA at temperatures ranging from 90–120 °C. Under these conditions, the cycloadduct was formed in high yields without breakdown of CMA simplifying the examination of the kinetics of this single step. The net rate of cycloadduct formation can be written as the forward rate of cycloaddition formation via Diels Alder reaction between CMA and ethylene minus the rate of the back reaction involving the retro Diels-Alder (rDA) of the cycloadduct. Assuming both of these reactions are elementary, the net rate can be written as that in equation 2. This equation can be simplified (Equation 3) based on the experimental conditions since ethylene was in ~10x excess, which was validated by plots of $\ln([CMA]_t/[CMA]_0)$ versus time all giving linear relationships (Figure S20 and S21 (MeCMA)). The experimental results and spectra (Figure 2) suggested that the rDA reaction had only a minimal contribution as (2) can be obtained with yields of 98 mol%, which further showed that $k_{1,DA} \gg k_{1,rDA}$ and justified the simplification of equation (3) into (4). DFT calculations also fully support this since ethylene addition is predicted to be highly exothermic (-127 kJ/mol).

$$-r_{CMA} = k_{1,DA}[CMA][Ethylene] - k_{1,rDA}[DAP] \quad (2)$$

$$-r_{CMA} = k'_{1,DA}[CMA] - k_{1,rDA}[DAP] \quad (3)$$

$$-r_{CMA} = k'_{1,DA}[CMA] \quad (4)$$

The observed rate constants at temperatures in the range of 90–120 °C are given in Table S4. The activation energy (E_A) for

the Diels-Alder reaction of CMA (or MeCMA) (depicted in Figure 3A) was calculated based on the slope of the Arrhenius plot shown in Figure 3B and Figure S21. The reaction of CMA and MeCMA with ethylene, resulted in a similar activation barrier of 77 kJ/mol. The experimental values were compared to the DFT-calculated barriers, which showed excellent agreement as the calculated enthalpic activation barriers were 67 and 68 kJ/mol, respectively. Therefore, the functionality

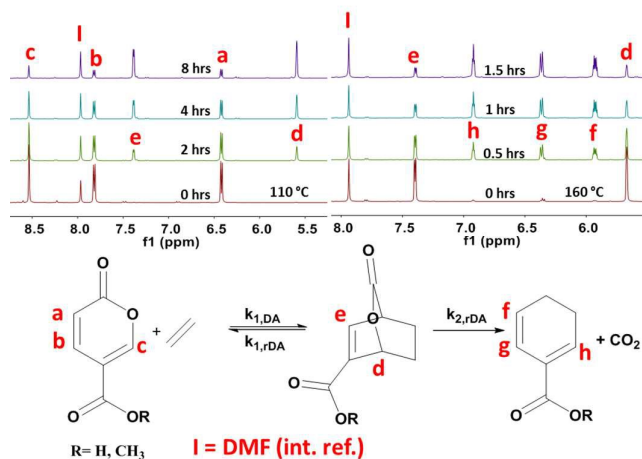


Figure 2. NMR trace of the Diels-Alder and decarboxylation reaction.

(acid or ester) had negligible influence on the 2-pyrone reactivity (Table S4). Literature reports for the cycloaddition of CMA derivatives and dienophiles with donating or withdrawing substituents report activation barriers that range from 28³⁴ to 118²¹ kJ/mol when using butyl vinyl ether or methyl acrylate, respectively. Given the nature of an inverse electron demand Diels-Alder cycloaddition, dienophiles with higher electron density from donating substituents should react more readily than dienophiles with electron withdrawing substituents.^{34, 35} With an activation barrier of 77 kJ/mol, the reaction of CMA (MeCMA) and ethylene showed that the unactivated dienophile resulted in intermediate Diels-Alder reactivity.

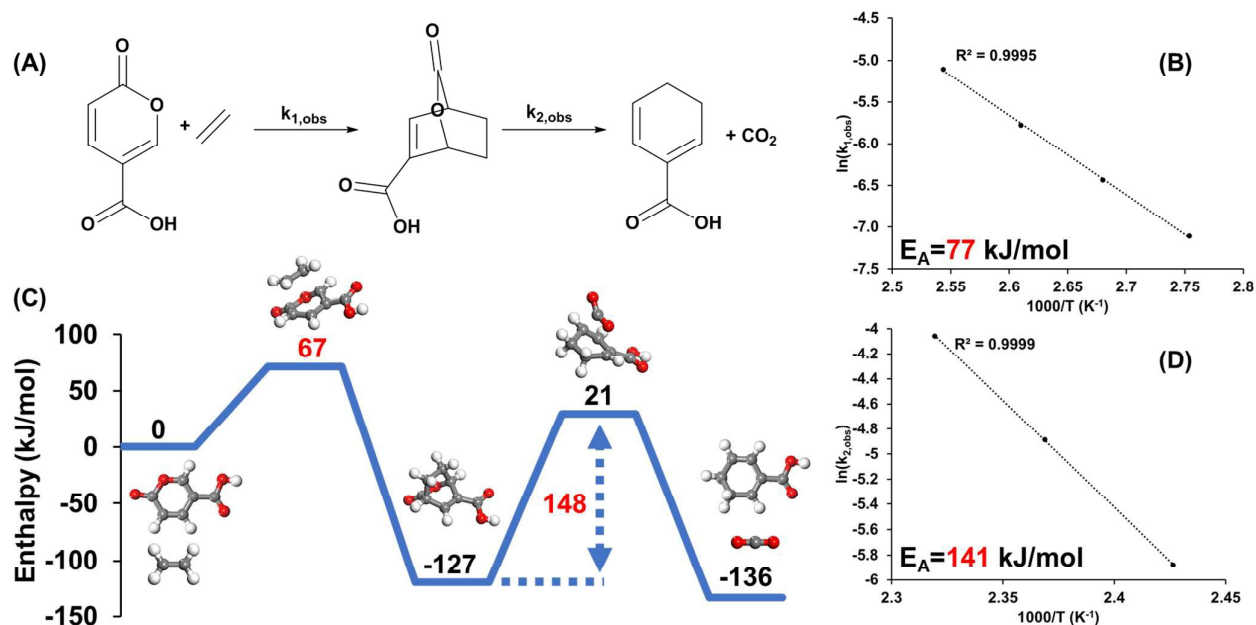


Figure 3. Network kinetic analysis of coumalic acid reaction with ethylene. (A) Diels-Alder reaction followed by thermal CO₂ extrusion. (B) Measured activation energy of the Diels-Alder reaction of CMA and ethylene in 1,4-dioxane at temperatures between 90–120 °C. (C) DFT-calculated reaction energy profile diagram for the CMA reaction with ethylene to the Diels-Alder adduct followed by decarboxylation to cyclohexa-1,5-diene carboxylic acid intermediate and CO₂. (D) Measured activation energy of the thermal decarboxylation reaction of CMA-DAP in 1,4-dioxane at temperatures between 140–150 °C.

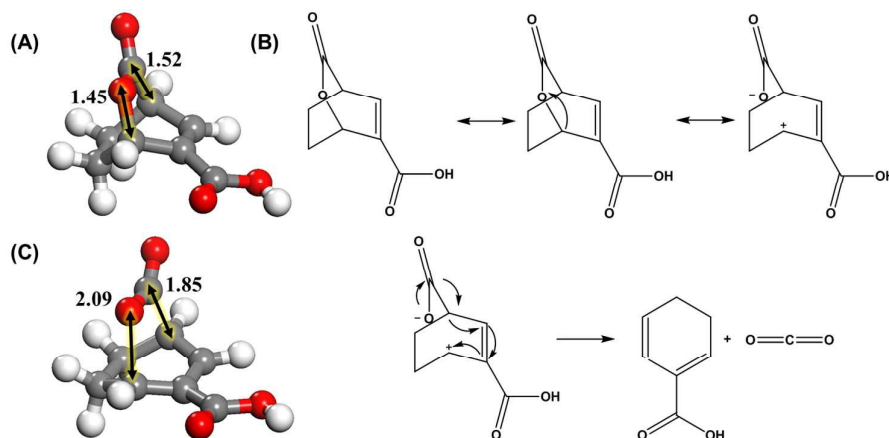


Figure 4. Bicyclic lactone decarboxylation. (A) Bond length (Å) of the cycloadduct of CMA and ethylene. (B) The asynchronous thermal decarboxylation mechanism of the CMA/ethylene Diels-Alder adduct to cyclohexa-1,5-diene carboxylic acid. (C) Bond length (Å) of the transition state of the cycloadduct CO₂ extrusion towards the cyclohexa-1,5-diene carboxylic acid with a more advanced C-O bond cleavage.

Decarboxylation reaction step

Examination of the bicyclic lactone (DAP) intermediate decarboxylation was carried out at temperatures ranging from 140–160 °C. The reactant, intermediate (2), was prepared using a 16 h reaction at 110 °C in 1,4-dioxane, which yielded almost pure DAP (2) with only trace amounts of intermediate (3) and unreacted (1). Decarboxylation reactions were performed using high pressure Wilmad-Labglass NMR tubes. The synthesized DAP (2) was dissolved in dioxane-*d*₈ within the tubes and the decarboxylation reactions as a function of time was measured via NMR (Figure 2).

The rate law for the decarboxylation step was assumed to follow unimolecular first order kinetics (Equation 5).

$$-r_{DAP} = k_{2,rDA}[DAP] \quad (5)$$

During the decarboxylation reactions, no accumulation of CMA (or MeCMA) was observed at any of the temperatures tested, which provided additional support that $k_{1,DA} \gg k_{1,rDA}$ and helped to validate the assumption that the equilibrium between CMA (or MeCMA) and DAP (2) was strongly shifted towards DAP formation. Plots of $\ln([DAP]_t/[DAP]_0)$ vs time resulted in linear trends for all temperatures tested (Figure S22–23).

The activation barriers for the decarboxylation of CMA/MeCMA-derived (2) (142/133 kJ/mol) were calculated based on the slope of the Arrhenius plots (Figure 3D and Figure S22) using the observed rate constants (Table S5). DFT calculations predicted an enthalpic activation barrier of 148 kJ/mol for both bicyclic lactones (CMA-DAP and MeCMA-DAP) as shown in Figure 3C. The DFT barriers agree well with those from experiment. Abdullahi et al. reported that the decarboxylation of the bicyclic lactone formed from ethyl coumalate and butyl vinyl ether also result in a high activation barrier of 111 kJ/mol which is also in close agreement with the DFT results that give a CO₂ extrusion barrier of 120 kJ/mol.³⁶ By comparing these results with our experimental activation energy, it is evident that the decarboxylation step is significantly influenced by the degree of functionalization of the bicyclic lactone intermediate. DFT energy mapping calculations (Figure 4) further suggested a mechanism where the CO₂-bridge leaves in an asynchronous fashion with a significantly elongated C-O bond in the transition state. As such, the C-O bond cleavage occurs prior to C-C bond cleavage, which is in agreement with observations from the literature.³⁶ From this analysis we conclude that the rate-limiting step in this reaction network is the decarboxylation reaction of (2). We observed that all reactions run with catalyst led to only minimal accumulation of (3), suggesting that the rate of (3) dehydrogenation is much more rapid than the rate of (3) formation. These results provide critical insight for what should be targeted to further enhance the overall process. Clearly, finding a catalyst to reduce the activation barrier of the rate-limiting decarboxylation would allow for this reaction to be carried out under milder reaction conditions, which would improve overall yields by reducing the extent to which by-products were formed.

Conclusions

In this work, we have shown that the Diels-Alder chemistry between CMA (or MeCMA) and ethylene can yield high conversion and selectivity towards BA (or MeBA), which provides a renewable alternative to current benzoate production. We were able to effectively elucidate the reaction network and revealed kinetic information such as activation energies for the Diels-Alder and the decarboxylation step. Although CMA stability studies revealed two independent break down pathways as a function of water concentration resulting in 2-butenal as the main by-product, the CMA decomposition rate was significantly slower than the Diels-Alder cycloaddition indicating that CMA stability is not a contributing factor. Instead, we have shown that the selectivity loss is a result of the formation of (4) and (6) and that in the presence of water intermediates on the pathway to BA led to by-product generation. Thus, the avoidance of water is critical to improve overall selectivity. Utilizing MeCMA gave diminished by-product formation, consequently improving benzoate selectivity.

Kinetic studies revealed that the activation barrier of the decarboxylation reaction was considerably higher than for the

Diels-Alder reaction, giving evidence that the extrusion of CO₂ is the rate limiting step, which is in agreement with DFT results. The high activation barrier of the CO₂ extrusion afforded the successful isolation of (2), granting access to bicyclic molecules in high yield and selectivity that could be utilized as synthetic starting substrates to synthesize a broad array of new compounds. For instance, we have shown that diene intermediates (3) from bicyclic lactones (2) can be accessed through controlled thermal extrusion of CO₂, providing access to novel molecules with dual-functionality. These insights can be leveraged to produce a plethora of products based on the coumalate conversion platform.

Experimental

Reagents and Materials

Coumalic acid (>97 %), γ -valerolactone (98 %), and 10 wt% Pd on activated carbon were obtained from Sigma Aldrich. Toluene (99.9 %), methanol (MS grade), water (MS grade), acetic acid (MS grade) were obtained from Fischer Scientific. Methyl coumalate (Acros Organics, 98 %), ethylene (99.5 %). The deuterated solvents benzene-*d*₆ (99.5 %), dioxane-*d*₈ (99.5 %) were obtained from Cambridge Isotope Laboratories Inc. All chemicals were used without further purification.

Apparatus and general procedure

Reaction kinetic measurements for the overall reaction of CMA (or MeCMA) and ethylene were performed using a 50 ml micro reactor system from Parr (4590 Series). Catalytic reactions were carried out using a 10 wt% Pd/C catalyst, which was added to the CMA (or MeCMA) containing solution before the reactor was sealed and purged five times with nitrogen to remove residual air. The reactor was then charged with ethylene for approximately 30 min until saturation of ethylene in the solvent was achieved. Subsequently, the system temperature was increased to the desired reaction condition with a heating rate of 10 K min⁻¹. Samples were periodically withdrawn from the reactor through a high pressure sampling tip tube to follow the reaction progress over time. Samples were withdrawn once the reactor reached the desired reaction temperature as the starting point reference. After the liquid phase reaction products were collected, the samples were filtered through a 0.2 micron syringe filter and analysed via NMR, UPLC-PDA/QDa and GC-FID/MS.

The Diels-Alder reaction evaluation of CMA or MeCMA with ethylene were performed at a temperature range between 90-120 °C without the presence of catalyst following the reaction procedure described above. The solvent 1,4-dioxane was used due to its superior solubility of both CMA and MeCMA.

The decarboxylation reaction studies of the Diels-Alder product (DAP) decarboxylation were performed at a temperature range between 140-160 °C, using high pressure NMR tubes from Wilmad-Labglass. The reactant (2) for this study was synthesized via Diels-Alder reaction of CMA (or MeCMA) and ethylene in 1,4-dioxane at 110 °C for 16 h giving high yield (>98 %). Through evaporation (using a stream of dry

air) of the solvent, the reaction product (2) was obtained and subsequently dissolved in dioxane-*d*8. The solution was then transferred into the high-pressure NMR tubes. Before the tube was sealed, 2.5 μ l of an internal standard (dimethyl formamid, DMF) was added to perform quantitative analysis. Subsequently, the tubes were placed into a heated oil bath to initiate the decarboxylation reaction. The tubes were periodically taken out of the oil bath cooled to room temperature and the reaction products were analysed via ^1H -NMR. Running the reaction in a deuterated solvent allowed for direct NMR sample analysis of the reaction products without further sample workup.

Reaction kinetics measurements of water mediated CMA breakdown was performed using different amounts of D_2O added to the solution comprising the deuterated solvent dioxane-*d*8 and the reactant CMA. This reaction was conducted using high pressure NMR tubes from Wilmad-LabGlass that were loaded with the reaction solution, sealed and heated without exposing the reaction solution to the gaseous reactant ethylene to exclusively investigate the stability of CMA under reaction conditions. Here, a 0.15 M stock solution of coumalic acid and 0.025 M solution of DMSO_2 (internal standard) was prepared in deuterated dioxane-*d*8. A total volume of 300 μ l of stock solution were added to the high pressure NMR tubes (Wilmad-Labglass) and H_2O or D_2O were added to yield 0-5 vol%. NMR tubes were sealed and heated to 171 $^\circ\text{C}$. Samples were removed and allowed to cool to room temperature prior to collection of ^1H NMR spectra.

To elucidate the reaction network of the MeCMA reaction with ethylene, 2D-NMR structural assignments were carried out using different NMR techniques such as ^1H -NMR, ^1H - ^1H COSY, ^{13}C - ^1H HSQC. The products analysed via 2D-NMR were obtained from the reaction of MeCMA and ethylene following a 48 h reaction at 90 $^\circ\text{C}$ in the absence of the Pd/C catalyst.

Sample analysis

NMR sample analysis of the reaction mixtures obtained from the batch reactions were carried out using a Bruker spectrometer equipped with a 14.1 Tesla superconducting magnet. The data were acquired and processed using TOPSPIN (version 3.0) and MestReNova (version 10.0.1-14719), respectfully. These samples were prepared using fully deuterated benzene-*d*6 or dioxane-*d*8, to both reduce the solvent background and as a species to use for field calibration. ^1H spectra were acquired using a recycle delay of 1.0 sec. and 30 $^\circ$ ^1H excitation pulse lengths. ^1H - ^1H 2D plots were acquired using a COSY pulse sequence, and ^{13}C - ^1H 2D plots were acquired using a HSQC pulse sequence.

Reaction products were also analyzed with ultra-pressure liquid chromatography (UPLC) using a Waters Acquity H-Class System equipped with a Photodiode Array (PDA) and a QDa mass detector. UPLC separation was carried out on a Waters BEH Phenyl column (2.1x100 mm, 1.7 μm particles). Additionally, samples were analyzed by GC using an Agilent 7890B gas chromatograph equipped with an Agilent DB-1701 column (60 m x 0.25 mm), a flame ionization detector (FID), and an Agilent 5977A mass spectrometer (MS). The methyl

ester version of (1), (3), (4), (5), and (6) were verified with NIST MS spectral library.

Computational

All of the calculations reported herein were performed using density functional theory with the M062X^{37, 38} hybrid functional as implemented in Gaussian 09³⁹. Optimizations were performed with a 6-311G+(d,p)⁴⁰ basis set on an ultrafine grid and tight convergence criterion for force. Solvation was modeled implicitly using the SMD model.⁴¹ Thermal corrections and partition functions were calculated within Gaussian at 298.15 K and subsequently used to calculate enthalpy and Gibbs free energies of all species. A factor of RT ln(24.46) was added to the free energies of all species to account for change of reference state from 1 atm to 1 M in solution. For degradation in water, additional corrections were applied corresponding to 55.56 M concentration of the bulk solvent.

Acknowledgements

We gratefully acknowledge funding from the National Science Foundation under Award EEC-0813570, the Iowa State University Chemical Instrument Facility staff members, and the Minnesota Supercomputing Institute (MSI) at the University of Minnesota. Furthermore, we would like to acknowledge all co-workers at CBiRC for their support.

References

1. R. L. D'Ecclesia, E. Magrini, P. Montalbano and U. Triulzi, *Energ. Econ.*, 2014, **46**, S11-S17.
2. E. Arceo, J. A. Ellman and R. G. Bergman, *ChemSusChem*, 2010, **3**, 811-813.
3. C. H. Christensen, J. Rass-Hansen, C. C. Marsden, E. Taarning and K. Egeblad, *ChemSusChem*, 2008, **1**, 283-289.
4. G. Fiorentino, M. Ripa and S. Ulgiati, *Biofuel, Bioprod. and Bior.*, 2016.
5. J. v. Haveren, E. L. Scott and J. Sanders, *Biofuel, Bioprod. and Bior.*, 2008, **2**, 41-57.
6. K. Wagemann, *ChemBioEng Reviews*, 2015, **2**, 315-334.
7. E. Mahmoud, J. Yu, R. J. Gorte and R. F. Lobo, *ACS Catal.*, 2015, **5**, 6946-6955.
8. World Health Organisation, Benzoic acid and Sodium benzoate. Concise international chemical assessment document, 26, 2000.
9. S. Ghosh, Y. Chisti and U. C. Banerjee, *Biotechnol. Adv.*, 2012, **30**, 1425-1431.
10. K. M. Draths, D. R. Knop and J. W. Frost, *J. Amer. Chem. Soc.*, 1999, **121**, 1603-1604.
11. S. K. Green, R. E. Patet, N. Nikbin, C. L. Williams, C.-C. Chang, J. Yu, R. J. Gorte, S. Caratzoulas, W. Fan, D. G. Vlachos and P. J. Dauenhauer, *Appl. Catal. B: Environ.*, 2016, **180**, 487-496.
12. J. J. Lee, G. R. Pollock Iii, D. Mitchell, L. Kasuga and G. A. Kraus, *RSC Adv.*, 2014, **4**, 45657-45664.

ARTICLE

Journal Name

13. S. H. Brown, L. Bashkirova, R. Berka, T. Chandler, T. Doty, K. McCall, M. McCulloch, S. McFarland, S. Thompson and D. Yaver, *Appl. microbiol. and biotech.*, 2013, **97**, 8903-8912.
14. R. M. Zelle, E. de Hulster, W. A. van Winden, P. de Waard, C. Dijkema, A. A. Winkler, J. M. Geertman, J. P. van Dijken, J. T. Pronk and A. J. van Maris, *Appl. Environ. Microbiol.*, 2008, **74**, 2766-2777.
15. S. J. Riley, Ph.D., Iowa State University, 2011.
16. T. Pfennig, R. L. Johnson and B. H. Shanks, *Green Chem.*, 2017.
17. J. J. Pacheco and M. E. Davis, *Proceedings of the Natl. Acad. Sci.*, 2014, **111**, 8363-8367.
18. S. Bérard, C. Vallée and D. Delcroix, *Ind. & Engin. Chem. Res.*, 2015, **54**, 7164-7168.
19. J. J. Lee and G. A. Kraus, *Green Chem.*, 2014, **16**, 2111-2116.
20. J. J. Lee and G. A. Kraus, *Tetrahedron Lett.*, 2013, **54**, 2366-2368.
21. G. A. Kraus, G. R. Pollock Iii, C. L. Beck, K. Palmer and A. H. Winter, *RSC Adv.*, 2013, **3**, 12721-12725.
22. G. A. Kraus, S. Riley and T. Cordes, *Green Chem.*, 2011, **13**, 2734-2736.
23. I. E. Markó, G. R. Evans, P. Seres, I. Chellé and Z. Janousek, *Pure Appl. Chem.*, 1996, **68**, 113-122.
24. G. H. Posner and Y. Ishihara, *Tetrahedron Letters*, 1994, **35**, 7545-7548.
25. N. P. Shusherina, *Russ. Chem. Rev.*, 1974, **43**, 851.
26. I. E. Markó and G. R. Evans, *Tetrahedron Lett.*, 1994, **35**, 2767-2770.
27. I. E. Markó and G. R. Evans, *Tetrahedron Lett.*, 1994, **35**, 2771-2774.
28. I. E. Markó, G. R. Evans and J.-P. Declercq, *Tetrahedron*, 1994, **50**, 4557-4574.
29. K. Afarinkia, V. Vinader, T. D. Nelson and G. H. Posner, *Tetrahedron*, 1992, **48**, 9111-9171.
30. M. Chia, M. A. Haider, G. Pollock, G. A. Kraus, M. Neurock and J. A. Dumesic, *J. Am. Chem. Soc.*, 2013, **135**, 5699-5708.
31. D. M. Alonso, S. G. Wettstein and J. A. Dumesic, *Green Chem.*, 2013, **15**, 584-595.
32. G. Strappaveccia, L. Luciani, E. Bartollini, A. Marrocchi, F. Pizzo and L. Vaccaro, *Green Chem.*, 2015.
33. D. Fegyverneki, L. Orha, G. Láng and I. T. Horváth, *Tetrahedron*, 2010, **66**, 1078-1081.
34. A. Corma and H. García, *Chem. Rev.*, 2003, **103**, 4307-4366.
35. F. Fringuelli and A. Taticchi, *The Diels-Alder Reaction: Selected Practical Methods*, Wiley, 2002.
36. M. H. Abdullahi, L. M. Thompson, M. J. Bearpark, V. Vinader and K. Afarinkia, *Tetrahedron*, 2016, **72**, 6021-6024.
37. Y. Zhao and D. G. Truhlar, *Journal Chem. Phys.*, 2006, **125**, 194101.
38. Y. Zhao and D. G. Truhlar, *Accounts Chem. Res.*, 2008, **41**, 157-167.
39. M. J. Frisch, G. W. Trucks, H. B. Schlegel, G. E. Scuseria, M. A. Robb, J. R. Cheeseman, G. Scalmani, V. Barone, B. Mennucci, G. A. Petersson, H. Nakatsuji, M. Caricato, X. Li, Hratchian, H. P., A. F. Izmaylov, J. Bloino, G. Zheng, J. L. Sonnenberg, M. Hada, M. Ehara, K. Toyota, R. Fukuda, J. Hasegawa, M. Ishida, T. Nakajima, Y. Honda, O. Kitao, H. Nakai, T. Vreven, J. A. Montgomery, Jr., Peralta, J. E., F. Ogliaro, M. Bearpark, J. J. Heyd, E. Brothers, K. N. Kudin, V. N. Staroverov, R. Kobayashi, J. Normand, K. Raghavachari, A. Rendell, J. C. Burant, S. S. Iyengar, J. Tomasi, M. Cossi, N. Rega, J. M. Millam, M. Klene, J. E. Knox, J. B. Cross, V. Bakken, C. Adamo, J. Jaramillo, R. Gomperts, R. E. Stratmann, O. Yazyev, A. J. Austin, R. Cammi, Pomelli, C., J. W. Ochterski, R. L. Martin, K. Morokuma, V. G. Zakrzewski, G. Voth, A., P. Salvador, J. J. Dannenberg, S. Dapprich, A. D. Daniels, O. Farkas, J. B. Foresman, J. V. Ortiz, J. Cioslowski and D. J. Fox, *Journal*, 2016, Gaussian 09, revision A.02, Gaussian, Inc.: Wallingford CT.
40. M. J. Frisch, J. A. Pople and J. S. Binkley, *J. Chem. Phys.*, 1984, **80**, 3265-3269.
41. A. V. Marenich, C. J. Cramer and D. G. Truhlar, *J. Phys. I Chem. B*, 2009, **113**, 6378-6396